Resonant Brillouin scattering in CdS. I. Experiment

J. Wicksted,* M. Matsushita,† H. Z. Cummins, T. Shigenari,‡ and X. Z. Lu
Department of Physics, City College of the City University of New York, New York, New York 10031
(Received 3 June 1983; revised manuscript received 31 October 1983)

High-resolution resonant Brillouin-scattering (RBS) experiments were performed in the vicinity of the A exciton in cadmium sulfide. The spectroscopic system used in these investigations consisted of a single-mode dye laser which was frequency tuned through the exciton resonance, and a triple-pass Fabry-Perot interferometer combined with a tandem grating spectrometer which was used to analyze the scattered light. This experimental arrangement enabled Brillouin shift, linewidth, and intensity measurements to be made on several different Brillouin components which result from the scattering by acoustic phonons of both inner- and outer-branch exciton-polaritons in the crystalline medium. Very good agreement was obtained between the Brillouin shift data and theory resulting in revised values for the exciton effective mass, transverse frequency, background dielectric constant, and oscillator strength. However, the Brillouin linewidth data indicated that the exciton damping constant Γ is not constant in value but instead increases monotonically for frequencies greater than ω_T. In an attempt to identify the correct additional boundary condition (ABC) which is needed to describe the simultaneous propagation of two degenerate exciton-polariton modes, a theoretical external scattering cross-section calculation was developed (see the following paper) and compared with the measured Brillouin intensities. Although the RBS intensity measurements did not fit very well with theory for any of the three ABC's, agreement between theory and experiment was considerably better with either ABC2 or ABC3 than with ABC1. The RBS results were also checked for self-consistency by reflectivity and absorption experiments on the same CdS sample.

I. INTRODUCTION

The existence in crystals of exciton-polaritons which are hybridized excitations of strongly interacting photons and dipole-active excitons was postulated in the late 1950s by Pekar[1] and by Hopfield.[2] The finite effective mass of the exciton results in the crystalline medium becoming spatially dispersive which leads to the simultaneous propagation of two degenerate exciton-polariton modes at frequencies above the exciton resonance. In order to properly describe the electrodynamics at the surface of this spatially dispersive medium, Maxwell's boundary conditions must be supplemented by an additional boundary condition (ABC).

During the 1960s and 1970s, extensive experimental and theoretical research was directed towards elucidating the properties of exciton polaritons and the ABC problem of spatially dispersive media. Much of the relevant work has been summarized recently in a collection of articles in Ref. 3.

In 1972, Brenig, Zeyher, and Birman (BZB) explored the consequences of treating exciton polaritons as intermediate states in Brillouin scattering at incident laser frequencies near an exciton resonance.[4] In contrast to resonant Raman scattering where the use of exciton polaritons as intermediate states leads to predictions which are hardly distinguishable from those using bare excitons,[5] spectacular changes in the predicted Brillouin spectrum were found. Because acoustic phonons exhibit linear ω-vs-k dispersion (in contrast to nearly dispersionless optical phonons), BZB found that (1) the Brillouin shifts should increase rapidly as the incident frequency is increased towards the exciton resonance from below, and (2) for frequencies above ω_L where both inner- and outer-branch polaritons can participate as intermediate states, a Brillouin octet representing all combinations of Stokes and anti-Stokes interbranch and intrabranch scattering would be present (see Fig. 1) in place of the Brillouin doublet seen below ω_L.

The analysis of BZB also produced several other predictions for the Brillouin scattering spectrum of semiconducting crystals near exciton resonances: (3) the linewidth of Brillouin components should increase as the resonance is approached, reaching a maximum near ω_T and should then decrease; (4) the relative intensities of the Brillouin components produced by the same type of acoustic phonon but with different intermediate polariton states depends critically on the choice of the ABC; and (5) variation of the intensity of a particular Brillouin component with incident laser frequency also depends strongly on the ABC.

The seminal paper of BZB led to numerous experimental studies which have confirmed many of their predictions. Resonant Brillouin scattering (RBS) has been studied in GaAs, CdTe, ZnSe, CuBr, CdS, CdSe, and HgI_2, and has been reviewed by Yu,[6] Ulbrich and Weisbuch,[7] and most recently by Koteles.[8] Most experiments reported to date have employed grating spectrometers to analyze the scattered light. However, the resolution of these spectrometers has usually been too low to permit observation of the Brillouin components resulting from inner-branch polariton scattering (1-1′ in Fig. 1), or of the Brillouin

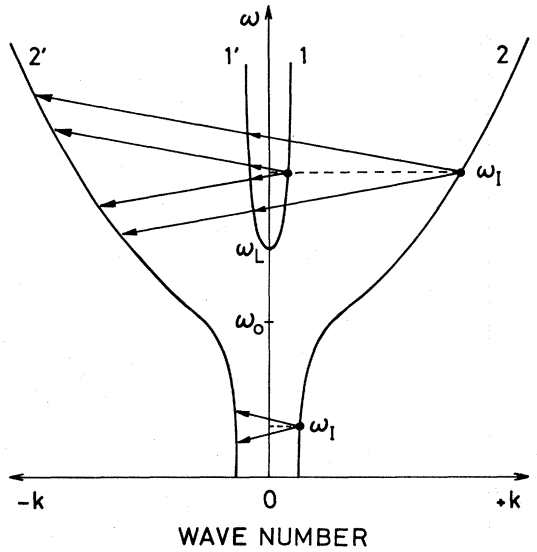

FIG. 1. Schematic representation of the kinematics of a Brillouin backscattering experiment. The incident photon (ω_I) creates a polariton propagating in the $+\vec{k}$ direction. A one-phonon scattering event creates a polariton propagating in the $-\vec{k}$ direction, simultaneously either creating (Stokes) or annihilating (anti-Stokes) a phonon. For $\omega_I < \omega_L$, only two scattered polaritons are possible. For $\omega_I > \omega_L$, the existence of two polariton branches gives rise to eight scattered polaritons, indicated by the tips of the arrows.

linewidths. Furthermore, all of the experiments with the exception of Yu and Evangelisti's study of CdS have concentrated on kinematics (mapping out the polariton dispersion curves), and have ignored the quantitative study of cross sections required for investigation of the ABC problem.[9]

We have undertaken an experimental investigation of resonant Brillouin scattering in CdS using a high-resolution spectrometer consisting of a triple-pass Fabry-Perot interferometer in series with a tandem grating spectrometer. The composite spectrometer allowed us to observe the previously undetected Brillouin components arising from inner-branch (1-1') scattering as well as the increase in Brillouin linewidth with increasing laser frequency. Preliminary results of this experiment were presented in a previous paper.[10] In this paper we present our complete results for Brillouin shifts and linewidths, and for the frequency-dependent cross sections.

In Sec. II we present a brief review of previous experimental studies of resonant Brillouin scattering in CdS followed by a description of our apparatus and experimental procedures in Sec. III. In Sec. IV we present our results and compare them to theoretical predictions, and in Sec. V we discuss the results and give our conclusions. A full discussion of the theory used in our data analysis is presented in the following paper.

II. SUMMARY OF PREVIOUS RBS EXPERIMENTS ON CdS

The crystal in which Raman and Brillouin scattering have been most extensively studied in the region of an exciton resonance is the II-VI wurtzite-structure semiconductor CdS. Even prior to the RBS predictions by BZB, Pine[11] had investigated resonant effects in the Brillouin spectrum of CdS by temperature tuning the $1S$ A exciton toward a fixed-frequency (6328-Å) laser. He observed a strong resonant enhancement in the LA Brillouin cross section as the frequency of the exciton was lowered (via increasing crystal temperature) towards the laser frequency. This temperature tuning technique was also utilized by Bruce and Cummins,[12] who observed both the strong resonant dispersion predicted by BZB and resonant enhancement of the LA Brillouin component as the A-exciton frequency was lowered toward the 4880-Å line of an argon laser. However, the additional features predicted by BZB could not be observed due to severe broadening effects and decreasing intensity resulting from phonon-assisted absorption at the temperature required to achieve resonance. Both of these studies used Fabry-Perot interferometry to analyze the scattered light.

In 1977, Winterling and Koteles utilized a tunable dye laser and grating spectrometer to perform RBS experiments in the region of the $n=1$ A- and B-exciton resonances in CdS at 4.2 K.[13] For the A exciton, both LA and TA phonons were observed in the backscattering geometry with incident laser wave vector perpendicular to the hexagonal c axis. Only intrabranch scattering involving the outer exciton-polariton branch (2-2') could be observed in these one-phonon scattering processes. Inner-branch participation, however, was ascribed to a two-phonon scattering feature which was observed when the incident laser frequency was above the longitudinal exciton frequency.[14] These two-phonon effects are possible because of the anisotropic and piezoelectric properties of CdS, the latter property also being responsible for the observation of the "forbidden" TA phonon which was first observed in CdS.[15] The B exciton was also investigated by this same group.[16] These RBS experiments proved to be extremely interesting since the B-exciton resonance was shown to exhibit either a two- or three-branch behavior for the incident laser light polarized either parallel or perpendicular to the crystal c axis. The three-branch behavior results from terms linear in wave vector in the B-exciton energy. As in the A-exciton case, both TA and LA one-phonon scattering was observed, although no two-phonon scattering processes were seen.

Yu and Evangelisti also carried out an investigation of RBS in CdS.[9] They considered the role of the ABC's in determining the cross section, as proposed by BZB, and suggested a new model for the CdS surface including, following Hopfield and Thomas,[17] a surface "dead layer" with a large damping constant. They found that the additional boundary condition ABC3 (see Sec. IV C of the following paper) gave the best fit to their LA 2-2' cross-section data with a 70-Å-thick lossy surface layer having $\Gamma' = 14\ \mathrm{cm}^{-1}$.

Flynn and Geschwind have investigated the linewidth of RBS in CdS. In a preliminary report of their results obtained with a multipassed Fabry-Perot interferometer and CdS platelets immersed in superfluid helium, they give maximum linewidths of 400 and 250 MHz for 2-2' scattering of LA and TA phonons, respectively.[18] We will

return to a discussion of these narrow linewidths in Sec. V.

Broser and Rosenzweig have recently performed RBS experiments on CdS while the crystal was subjected to high magnetic fields ($\vec{H}\perp\hat{c}$).[19] Owing to the field-induced mixing and splitting of the allowed Γ_5^T and forbidden Γ_6 states of the A exciton, a three-polariton-branch model was required to fit the Brillouin shift data. The LA Stokes line corresponding to outer-branch scattering at $H=0$ was seen to split into three sublines with increasing magnetic field. For a fixed field, the Brillouin shifts of these three lines were theoretically fitted by considering interbranch and intrabranch LA-phonon scattering between the two outer polariton branches only. These fits resulted in the determination of the singlet (Γ_5^T)—triplet (Γ_6) energy splitting. Corresponding splitting of the TA Stokes line could not be resolved in these experiments. Rosenzweig has also described his efforts to extract information on the ABC problem from these experiments. He concludes that different kinds of experiments (RBS, reflectivity, and transmission) seem to suggest different ABC's.[20]

III. EXPERIMENTAL DESIGN AND PROCEDURE

A. Experimental design

The experimental arrangement used for the RBS studies is shown in Fig. 2. A Spectra Physics model no. 171 krypton-ion laser operating in the deep blue (4067—4226 Å) with an output power between 2.0 and 2.5 W was used to pump a Coherent Radiation model no. 590 dye laser using coumarin 102 dye. Selection of a single mode from the broad dye fluorescence bandwidth (4700—5150 Å) was achieved using the intracavity combination of a quartz birefringent filter and double-etalon assembly consisting of thick (1-cm) and thin (0.5-mm) fused-quartz etalons. The single-frequency output of the dye laser could be quasicontinuously tuned in frequency increments of 0.3 cm^{-1} over a frequency range of 19 600—21 200 cm^{-1}.

Certain instabilities in the output-frequency spectrum of the dye laser complicated the RBS experiments, the most important of which was the fluctuation of the output power which induced thin-etalon mode hopping. This problem was partially alleviated by incorporating a Spectra Physics model no. 373 dye-laser light stabilizer into the experimental setup which maintained a dye-laser output of 15 mW. However, mode hops still occurred on the average of one every 5 min. Thus the output spectrum of the dye laser had to be continuously monitored by a Coherent model no. 470 optical-spectrum analyzer so that undesirable modes could be eliminated through the tilting of the thin etalon. The light was then passed through a polarization rotator to obtain the desired polarization before being focused onto the CdS sample. A backscattering geometry was used with both the wave vector and polarization of the incident laser light perpendicular to the crystal c axis ($\vec{k}\perp\hat{c}$,$\vec{E}\perp\hat{c}$).

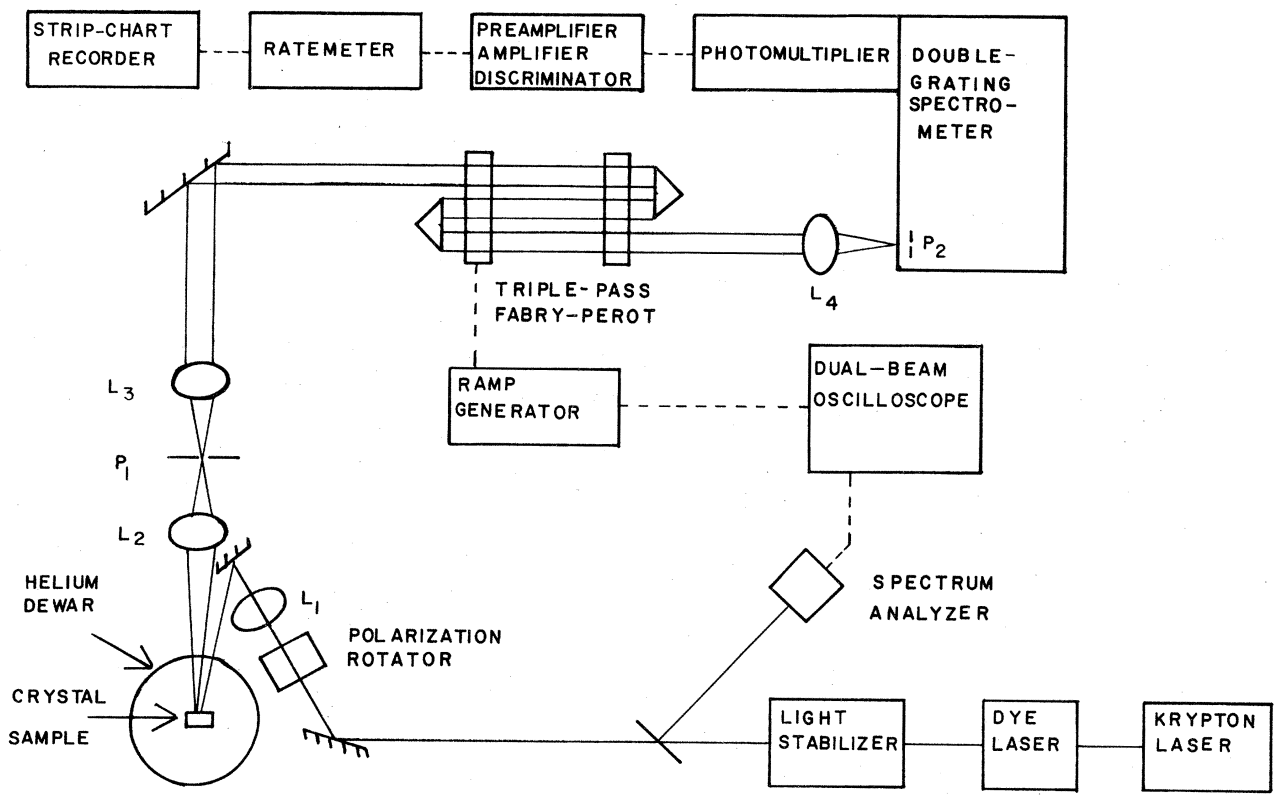

FIG. 2. Schematic of RBS experimental arrangement. L_1, L_2, L_3, and L_4 are sample focusing, pinhole focusing, Fabry-Perot collimating, and spectrometer focusing lenses, respectively. Focal lengths of these lenses are 13, 5.5, 5.5, and 18.7 cm, respectively. Pinholes P_1 and P_2 have diameters of 200 and 150 μm, respectively.

The CdS platelets were vertically attached to a hexagonally shaped copper sample mount via a conductive vacuum grease mixture consisting of Air Products Crycon and Apiezon *N*-grease. The sample mount was then placed inside a Janis "supervaritemp" liquid-helium Dewar (model no. 8DT), which allowed optical access. Cooling of the sample was obtained by helium exchange gas flowing over the copper sample mount and by conduction between the sample and the mount. Most RBS experiments were performed at 4.2 K although occasionally the liquid helium was allowed to fill the sample space and was pumped to obtain temperatures of 2.7 K.

Light scattered by the sample was collected and focused onto a pinhole by a camera lens. A second lens then collimated the light emitted from the pinhole which acted as a point source for a Burleigh Instruments model no. RC-110 triple-pass piezoelectric Fabry-Perot interferometer. This interferometer used two plane mirrors which were coated for 93% reflectivity in the spectral region 4500—5500 Å. Its finesse varied between 40 and 60 with a contrast $\sim 1\times 10^{6}$.[21] The free-spectral range (FSR) of the interferometer was measured by scanning over the dye-laser output with two thin-etalon modes ($\Delta\nu \sim 6.7$ cm^{-1}) present.

The light emerging from the ramped Fabry-Perot interferometer was focused into a $\frac{3}{4}$-m Spex model no. 1401 double-grating spectrometer which served two purposes: (i) It determined the incident dye-laser frequency by scanning over the scattered Rayleigh light, and (ii) it acted as a tunable laser filter allowing only Rayleigh and Brillouin components to pass during the interferometer scan. Light leaving the spectrometer was focused onto the cathode of a cooled ITT FW 130 photomultiplier tube whose output was processed with photon-counting electronics and recorded on a strip-chart recorder, or alternatively multiscaled into a PDP-8E minicomputer.

The samples used in the RBS experiments were vapor-grown single-crystal CdS platelets generously provided by Wright-Patterson and General Motors (GM). The crystals, with the crystallographic *c* axis in the plane of the sample, had typical surface-area dimensions of 3×5 mm^2 with thicknesses $\sim 10^{-2}$ cm. In a preliminary study, the reflectivity, absorption, and luminescence spectra of these CdS platelets were investigated.[22] The GM platelets exhibited a much weaker bound exciton luminescence (*I* lines) indicating a lower concentration of impurities and defects, and were therefore used predominantly in the RBS experiments. We noted, however, that the strength of bound exciton luminescence was not clearly correlated with the sharpness of the *A*-exciton feature in the reflectivity spectrum which was particularly narrow in some of the Wright-Patterson platelets despite strong bound exciton luminescence.

B. Experimental procedure

The experimental procedure will now be described.[10] The dye laser was first tuned to some frequency in the vicinity of the *A* exciton in CdS ($\sim 20\,588$ cm^{-1}). The output of the 8-GHz optical-spectrum analyzer was displayed on the oscilloscope in order to verify that the dye-laser output consisted of a single frequency. The laser frequency was determined by allowing the Fabry-Perot interferometer to quickly ramp through its FSR with a ramp duration of 20 msec. Since the elastic Rayleigh component is dominant in the output of the Fabry-Perot interferometer, the laser frequency can be obtained by slowly scanning the grating spectrometer with narrow slitwidths over this elastic component. The slow scan (7.5 cm^{-1}/min) allowed the experimenter to mark the strip-chart record in 1-cm^{-1} intervals by visual comparison with the spectrometer wave-number indicator. Subsequent interpolation between the 1-cm^{-1} marks allowed the laser frequency to be determined to the nearest 0.1 cm^{-1}. Measurements made in this way were reproducible to about 0.2 cm^{-1}. After the frequency was determined, the spectrometer slits were opened to provide a passband slightly larger than the FSR of the Fabry-Perot interferometer. The gratings of the spectrometer were then positioned so that either the Stokes or anti-Stokes Brillouin components would be passed by the spectrometer. The interferometer was then scanned through its FSR in ~ 100 sec and the output of the combined Fabry-Perot-spectrometer system was recorded on a strip-chart recorder. The frequency of the dye laser was then changed by tilting the thin etalon as previously described, and the above procedure was then repeated. The end result was a series of Stokes and anti-Stokes Brillouin spectra for a range of dye-laser frequencies near the *A* exciton.

Figure 3 gives an illustrative comparison between the RBS spectra obtained with the combined Fabry-Perot interferometer-grating spectrometer system using the procedure described above, and the spectra obtained with a scanning grating spectrometer alone, the latter technique having been used in most of the previous RBS experiments. The Stokes [Fig. 3(b)] and anti-Stokes [Fig. 3(c)] TA(2-2′) components are clearly resolved when the combined system is used (effective resolution ~ 0.15 cm^{-1}) whereas the spectra recorded by the grating spectrometer alone [Fig. 3(a)] shows Stokes TA components which are not completely resolved while the anti-Stokes TA components are obscured by the wing of the Rayleigh line.

The FSR of the Fabry-Perot interferometer was chosen in such a way that the Brillouin components resulting from the scattering process could easily be observed. For example, to observe intrabranch scattering from the upper polariton branch (i.e., 1-1′ scattering), a FSR equal to 2.11 cm^{-1} was used.

IV. RESULTS

A. Brillouin shifts

Two illustrations of the Stokes Brillouin spectra are given in Figs. 4 and 5 with the FSR of the Fabry-Perot interferometer equal to 12.63 and 2.11 cm^{-1}, respectively. These illustrations clearly show (1-2′) and (2-1′) interbranch and (1-1′) intrabranch acoustic-phonon scattering processes which have not been observed in previous RBS experiments on CdS.[13,15]

Figure 6 shows all the observed one-phonon Brillouin shifts obtained from a single CdS crystal sample (GM no.

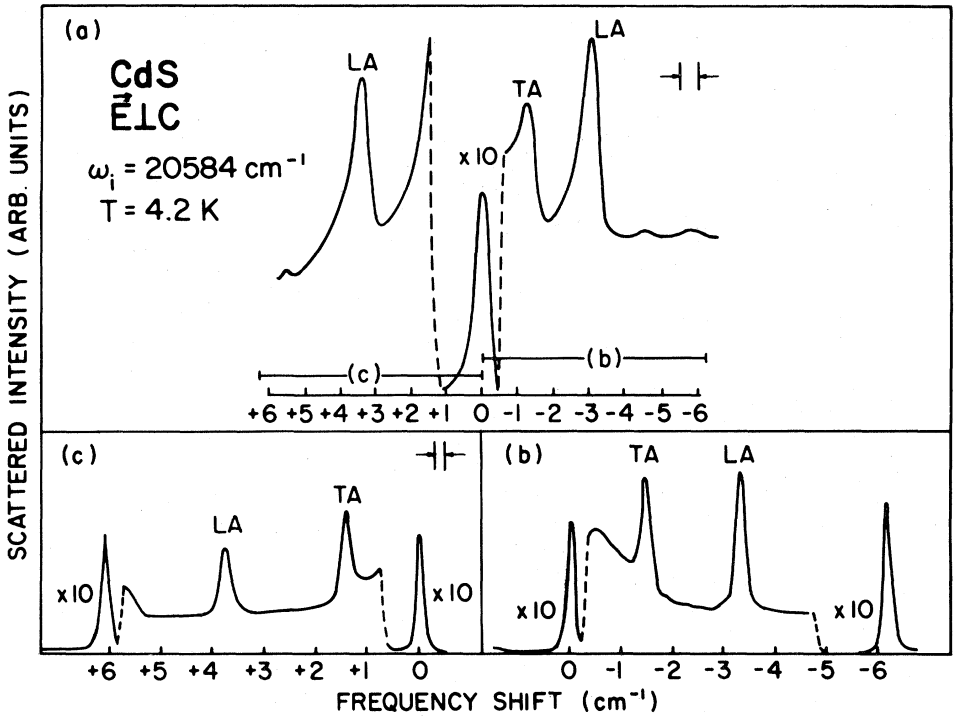

FIG. 3. Brillouin spectrum of CdS with $\omega_I = 20\,584$ cm^{-1}, analyzed with (a) double-grating spectrometer alone; (b) and (c) Fabry-Perot interferometer and grating spectrometer in series. For the Stokes (b) and anti-Stokes (c) high-resolution spectra, the FSR of the interferometer was 6.1 cm^{-1} and the grating slits were adjusted to give the passband indicated in (a). The Brillouin components result from LA(2-2′) and TA(2-2′) scattering.

21E-2). Three FSR's of the interferometer were employed: 2.11, 5.87, and 12.63 cm^{-1}. The solid lines through the data points represent the best fit of the theoretical Brillouin shift given in the following paper by Eq. (3.34) to the data by a nonlinear least-squares-fitting procedure. (Note that all equations referred to in this paper are from the following theoretical paper.) The four exciton parameters resulting from the fit, along with the longitudinal and transverse sound velocities used are listed in Table I. Also included in this table are the best fits ob-

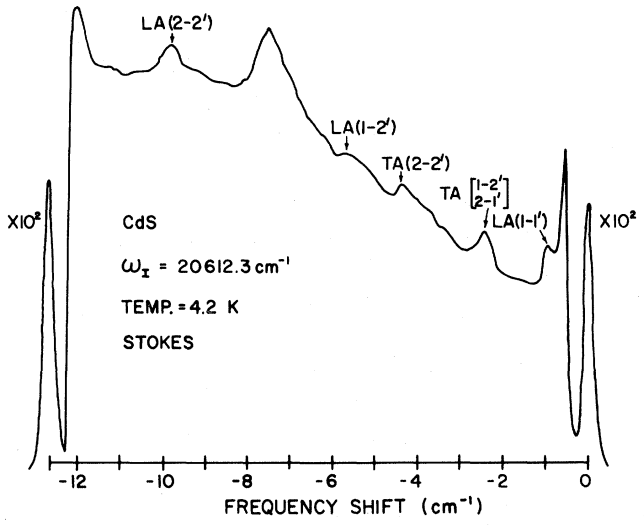

FIG. 4. Brillouin spectrum of CdS with $\omega_I = 20\,612.3$ cm^{-1}. The Fabry-Perot interferometer FSR was 12.63 cm^{-1} with the spectrometer set to pass Stokes Brillouin components. These one-phonon components result from LA(1-1′), TA($^{1-2'}_{2-1'}$), TA(2-2′), LA(1-2′), and LA(2-2′) scattering. The large unlabeled peak is due to two-phonon scattering.

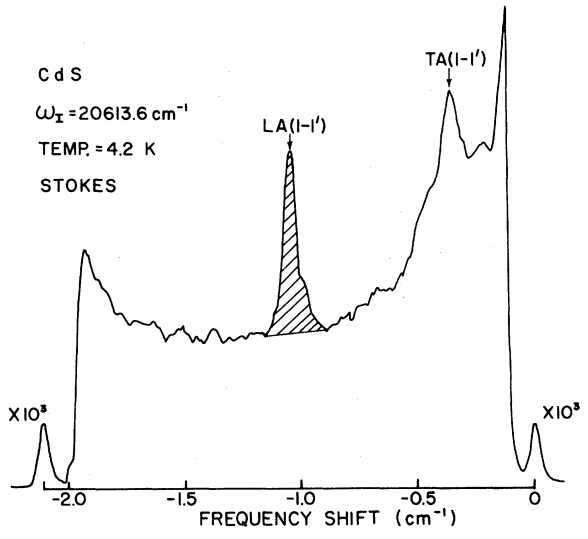

FIG. 5. Brillouin spectrum of CdS with $\omega_I = 20\,613.6$ cm^{-1}. The Fabry-Perot interferometer FSR equaled 2.11 cm^{-1} with the spectrometer set to pass Stokes Brillouin components. These Brillouin components result from LA(1-1′) and TA(1-1′) scattering. Hatched region of the LA(1-1′) component represents the area measured by a planimeter for determining the experimental scattering cross section.

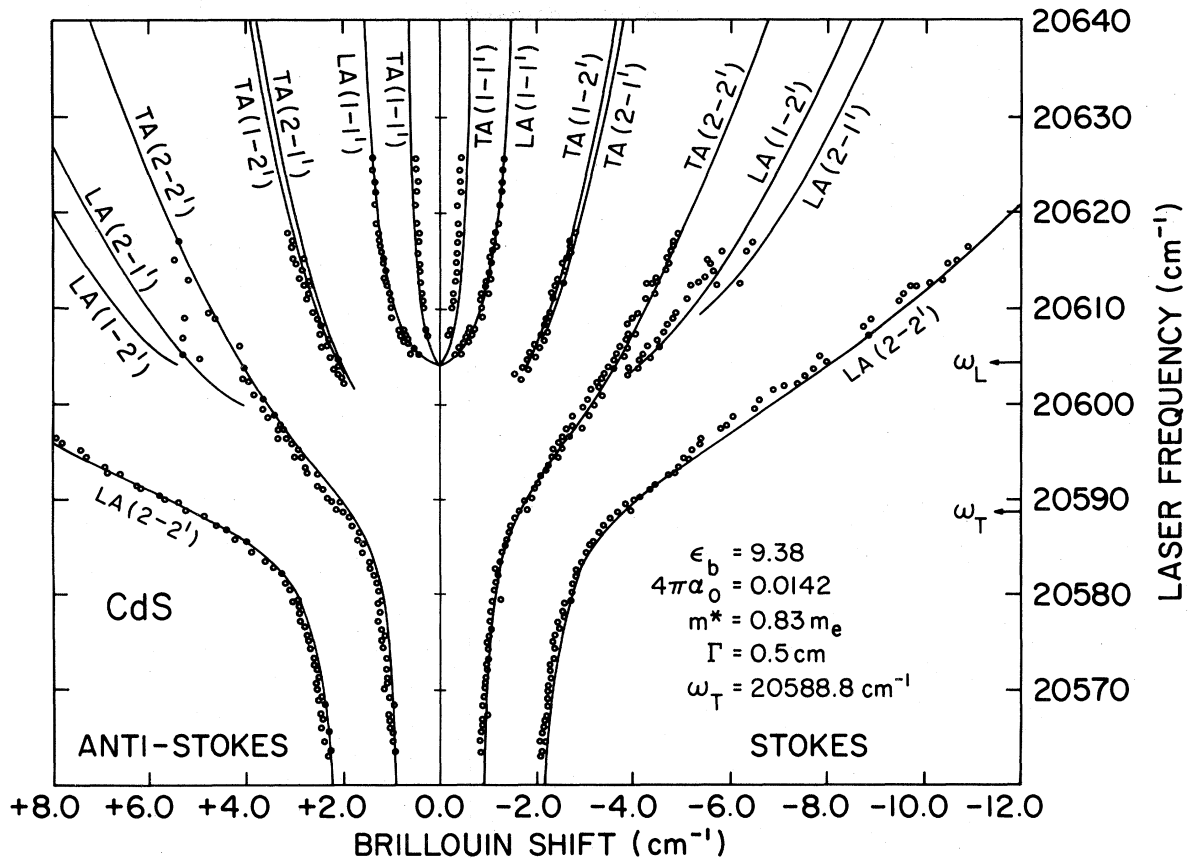

FIG. 6. Brillouin shifts of observed one-phonon Stokes and anti-Stokes peaks as a function of incident laser frequency. Experimental Brillouin shift data were obtained by using three different FSR's of the Fabry-Perot interferometer (2.11, 5.87, and 12.63 cm^{-1}). Solid lines represent the best fit of the theoretical Brillouin shift to the data.

tained by Winterling and Koteles.[23] It should be noted that the theoretical Brillouin shifts are independent of the exciton damping constant Γ (chosen here to be 0.5 cm^{-1}) for $0 \leq \Gamma < 5$ cm^{-1}.

B. Brillouin linewidths

The theoretical analysis of BZB predicted that the linewidth of the Brillouin components should increase as the incident laser frequency approaches the exciton resonance from below.[4] The exciton damping constant Γ in the polariton dispersion relation [Eqs. (3.6) and (4.1)] is responsible for the linewidth increase of these components. Broadening of both the LA(2-2') and TA(2-2') components was observed in the RBS experiments. Figure 7 shows the approximate full width at half maximum (FWHM) Δ of the Stokes TA(2-2') components determined by subtrac-

TABLE I. Best-fit values of the exciton parameters for the $n=1$ A exciton in CdS.

Parameter	Current values	Winterling and Koteles[a]
Dielectric constant		
ϵ_b	9.38	
Effective mass		
m^*	$0.83m_e$	9.3
Oscillator strength		
$4\pi\alpha_0$	0.0142	$0.89m_e$
Transverse frequency		
ω_T	20588.8 cm^{-1}	0.0139
Sound velocities[b]		
$c_{s_{LA}}$	4.25×10^5 cm/sec	20589.5 cm^{-1}
$c_{s_{TA}}$	1.76×10^5 cm/sec	

[a]G. Winterling and E. S. Koteles, in *Lattice Dynamics,* edited by M. Balkanski (Flammarion, Paris, 1978), p. 170.

[b]D. Gerlich, J. Phys. Chem. Solids 28, 2575 (1967).

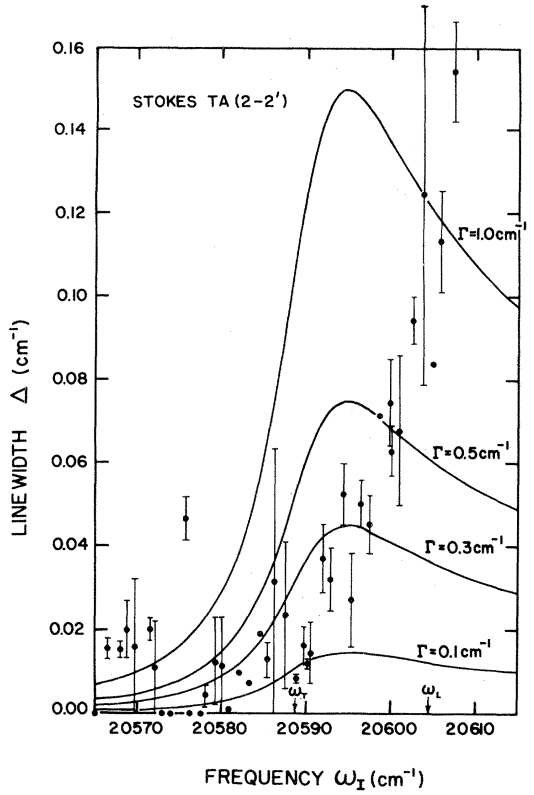

FIG. 7. Approximate experimental linewidths of the Stokes TA(2-2') Brillouin components (FWHM with laser linewidth subtracted) as a function of incident laser frequency. The solid lines are theoretical predictions with four different values of the exciton damping parameter Γ.

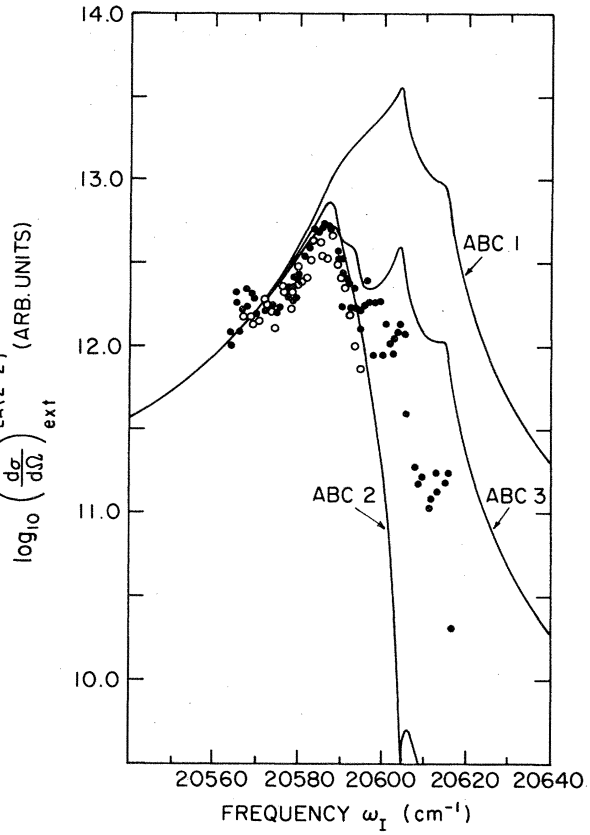

FIG. 8. $\log_{10}$ comparison of the theoretical external scattering cross section for the Stokes LA(2-2') scattering for various ABC's with the $\log_{10}$ of the experimentally measured Brillouin intensity. Open (closed) circles represent the data which have been obtained with a FSR equal to 5.87 cm^{-1} (12.63 cm^{-1}). Both sets of data have been normalized to the curves in the frequency region $20\,560 \leq \omega_I \leq 20\,570$ cm^{-1}.

tion of the instrumental linewidth (FWHM of the Rayleigh line) from the Brillouin linewidth at each laser frequency (some of the data were digitally recorded after which both the Rayleigh and Brillouin components were fitted to Lorentzian line shapes). Additional broadening of the TA Brillouin components due to finite collection angle effects was estimated to be less than 10^{-4} cm^{-1}.[21] The solid curves in Fig. 7 are the theoretical predictions[4] with four different values of Γ [see Eq. (3.35)]. The curves were computed using values of the exciton parameters determined from the Brillouin shifts (Table I) and with Γ taken as a frequency-independent constant. However, $\Gamma(\omega)$ may be an increasing function of ω for $\omega > \omega_T$, as suggested by Cho,[24] which would improve the agreement between experiment and theory.

C. External scattering cross sections

In Fig. 8, the logarithm of the intensity of the Stokes LA(2-2') Brillouin components resulting from RBS experiments utilizing two different FSR's of the Fabry-Perot interferometer are shown along with the three theoretical external scattering cross sections. The three theoretical curves result from Eq. (3.36) with $\Gamma_0(q)$ given by Eq. (4.17) and $T_i(\omega_I)$ and $T_j'(\omega_s)$ computed via Eqs. (4.12) and (4.13) for the three different ABC's [Eq. (4.8)]. The data in this figure have been normalized in the frequency region where the three theoretical curves are approximately equal ($20\,560 \leq \omega_I \leq 20\,570$ cm^{-1}). The normalization constant for the data obtained using a FSR equal to 12.63 cm^{-1} (closed circles) was ~ 8.2 while the normalization constant for the data obtained with FSR equal to 5.87 cm^{-1} (open circles) was ~ 8.54. Each data point was determined by measuring the actual Brillouin line area from the strip-chart record using a planimeter. The equation used to determine the intensity of each Brillouin line is (before taking the logarithm)

$$I = A\left[\frac{\Delta\omega_{\mathrm{FSR}}}{L}\right]\left[\frac{R}{100}\right].$$

Here A is the averaged area of the Brillouin component as measured several times with the planimeter (see Fig. 5 for an illustration of the area measured), $\Delta\omega_{\mathrm{FSR}}$ is the FSR of the Fabry-Perot interferometer (in cm^{-1}), L is the physical distance on the chart between the two Rayleigh lines and R is the full scale reading of the ratemeter (in counts/sec).

A similar illustration for the intensity of the Stokes TA(2-2') data with the FSR equal to 5.87 cm^{-1} is given in Fig. 9. Each data point here has been normalized by the same normalization constant (~ 8.54) used for the Stokes LA(2-2') data recorded with FSR equal to 5.87 cm^{-1} (open circles in Fig. 8). The three curves in Fig. 9

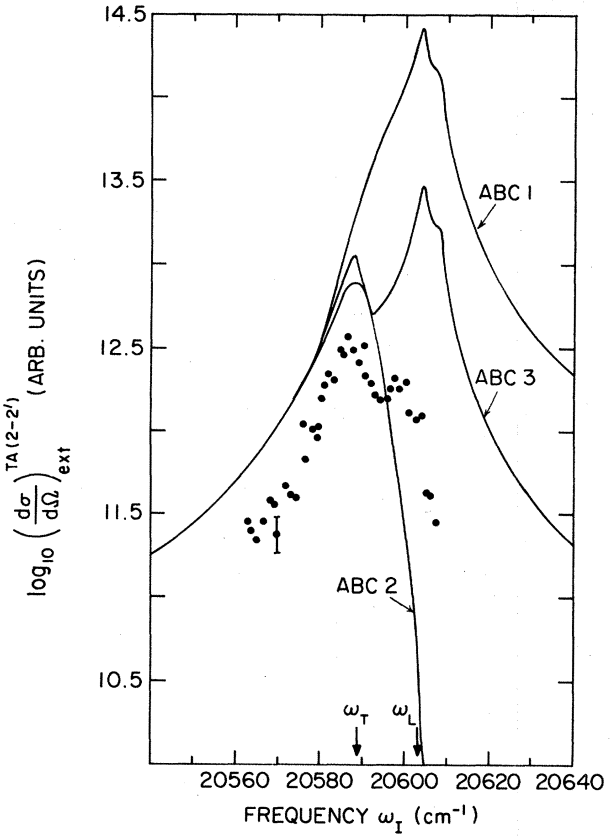

FIG. 9. $\log_{10}$ comparison of the theoretical external scattering cross section for the Stokes TA(2-2') scattering for various ABC's with the $\log_{10}$ of the experimentally measured Brillouin intensity. The closed circles represent the data which have been obtained via a FSR equal to 5.87 cm^{-1}. This data has been normalized by the same constant used for the open circle data in Fig. 8.

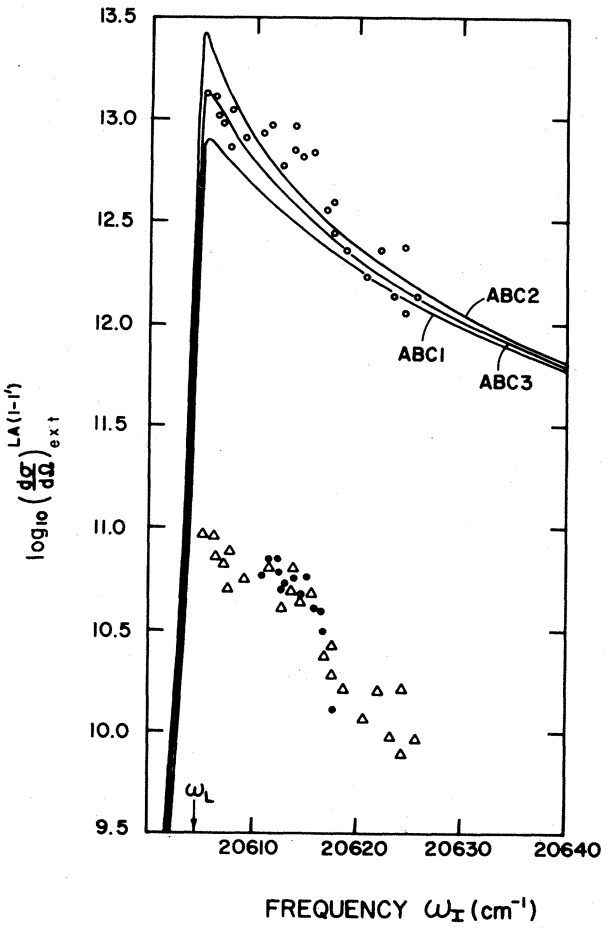

FIG. 10. $\log_{10}$ comparison of the theoretical external scattering cross section for the Stokes LA(1-1') scattering for various ABC's with the $\log_{10}$ of the experimentally measured Brillouin intensity. Open circles plotted along the theoretical curves represent data which have been normalized to the theory ($\Delta\omega_{FSR}=2.11$ cm^{-1}). Closed circles represent data which have been normalized by the same constant used for the Stokes LA(2-2') data in Fig. 8 with $\Delta\omega_{FSR}=12.63$ cm^{-1}. The open triangles represent data obtained with $\Delta\omega_{FSR}=2.11$ cm^{-1} which have now been normalized to the closed circle data.

represent the external scattering cross sections for the three ABC's in the case of the piezoelectric polariton-phonon interaction [Eq. (4.18)].

The logarithm of the intensities of the Stokes LA(1-1') Brillouin lines obtained using two FSR's equal to 2.11 and 12.63 cm^{-1} are shown in Fig. 10 along with the three theoretical scattering cross-section curves obtained from Eq. (3.36) with $\Gamma_0(q)$ given by Eq. (4.17). The open circles are the data with FSR$=2.11$ cm^{-1} which have been normalized to the theoretical curves. The solid circles and open triangles represent data obtained from two FSR's equal to 12.63 and 2.11 cm^{-1}, respectively, which have been normalized by the same normalization constant (~ 8.2) used for the Stokes LA(2-2') with FSR$=12.63$ cm^{-1}.

D. Absorption and reflectivity

In order to test the self-consistency of the exciton parameters and ABC's, we also performed absorption and reflectivity studies of the same CdS samples used in the RBS experiments. The absorption measurements were performed at 4.2 K over the frequency region $20\,540 \leq \omega_I \leq 20\,670$ cm^{-1} ($\vec{k}_I \perp \hat{c}$, $\vec{E}_I \perp \hat{c}$). The experiment utilized the dye laser to vary the incident frequency over this region. The intensity of the light transmitted through the crystal, and the intensity of a reference beam used to correct for equipment variations at different laser frequencies, were measured by scanning the grating spectrometer over the incident laser frequency. It was noticed, however, that small depolarization effects from the polarization rotator and the fused-quartz Dewar windows resulted in the incident polarization having a small component parallel to the c axis, and thus yielding a larger transmission through the sample. A small polarizer was therefore placed inside the helium Dewar to ensure a maximum incident polarization perpendicular to the c axis.

The theoretical calculation of the optical density is performed by taking the intensity ratio of the light transmitted through the crystal to the incident laser light

$$\frac{I_T^{ext}}{I_I^{ext}} = \sum_{i=1}^{2} T_i(\omega_I)\exp(-2k_i''L)T_i'(\omega_I)\ ,$$

where $T_i(\omega_I)$ and $T_i'(\omega_r)$ are given by Eqs. (4.12a),

(4.12b), and (4.13) (for $i=1$ and 2, respectively), k_{I_i}'' is the imaginary part of the ith polariton wave vector and L is the sample thickness. (Interference effects between the two propagating modes and multiple reflections from the sample surfaces have been neglected.) The curves resulting from this equation using ABC1 [Eq. (4.8)] are shown in Fig. 11 for six different values of Γ along with the experimentally measured optical densities for several different incident laser frequencies. The Γ value of ~ 0.05 cm^{-1} in the frequency region between 20 560 and 20 580 cm^{-1} seems to be the most appropriate one. This value of Γ should be considered as a lower bound since some light was probably transmitted through the crystal due to the depolarization effects mentioned earlier. Recently, however, Yu has measured the polariton luminescence following fast pulse excitation in platelets from the same lot of crystals used in our experiments and found an exciton lifetime of ~ 0.5 nsec,[25] suggesting $\Gamma \sim 0.01$ cm^{-1} which is considerably less than the lower limit set by our transmission measurements. This result will be further discussed in Sec. V.

Since we sought to obtain a self-consistent description of the electrodynamics of CdS, we also measured reflection spectra of our samples using a small tungsten lamp as the light source and the Spex grating spectrometer to analyze the reflected light (see Ref. 12 for details of the experimental procedure). The reflection spectra obtained exhibited the usual sharp feature at ω_T. A sharp spike was sometimes observed at ω_L but usually disappeared on repeated temperature cycling.

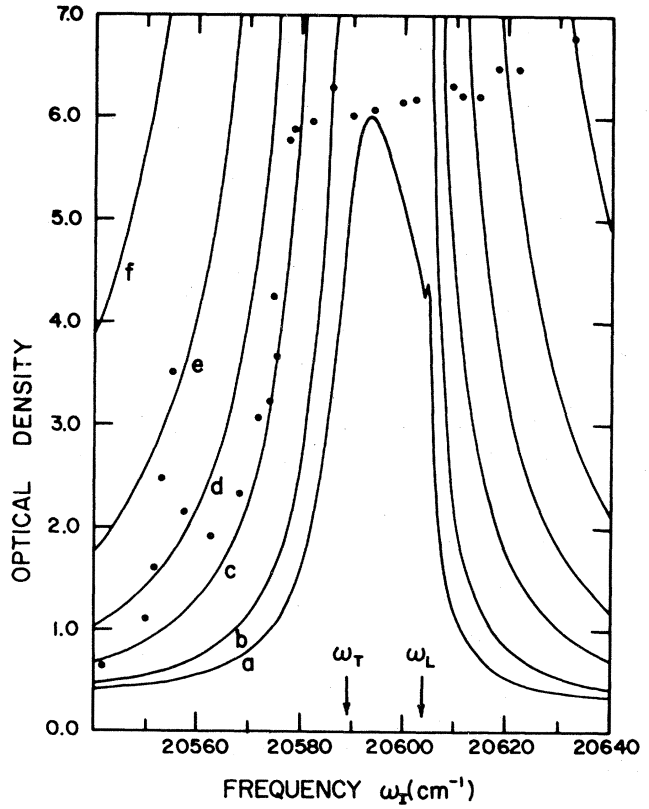

FIG. 11. Comparison between the theoretically calculated and experimentally measured optical densities. The theoretical optical-density expression utilizes transmissivity expressions from paper II using ABC1. Six values of Γ have been chosen: *a* $\Gamma=0.01$ cm^{-1}; *b* $\Gamma=0.02$ cm^{-1}; *c* $\Gamma=0.05$ cm^{-1}; *d* $\Gamma=0.1$ cm^{-1}; *e* $\Gamma=0.2$ cm^{-1}; *f* $\Gamma=0.5$ cm^{-1}; other parameters used are from Table I. (The peak in the optical density between 20 550 and 20 560 cm^{-1} is due to absorption by the I_2 bound exciton.)

The reflectivity spectra obtained with the same samples used in the RBS experiments were analyzed by including the full spatially dispersive form for the A exciton and treating the B exciton as dispersionless (infinite-mass approximation) [see Fig. 12(a)]. Fitting was restricted to the frequency region 20 654—20 482 cm^{-1} which includes the A-exciton resonance but not that of the B-exciton. Relatively poor fits were obtained with all three ABC's, and all indicated large Γ values (see Table II).

In view of the poor fits obtained, the analysis was repeated with the inclusion of an exciton-free dead layer at the crystal surface [Fig. 12(b)]. In this fit, all the exciton parameters except Γ were held fixed, and the fit was obtained by varying Γ, the background dielectric constant ϵ_b, and the thickness l and refractive index (assumed real) of the dead layer. Much better fits were obtained this time; however, the Γ values obtained for ABC2 and ABC3 were again unreasonably large as shown in Table II.

V. DISCUSSION AND CONCLUSIONS

The nonlinear least-squares fitting of the RBS theory to the Brillouin shift measurements resulted in revised values of the CdS A-exciton parameters: $4\pi\alpha_0$, m^*, ϵ_b, and ω_T (see Table I). These values were then incorporated into the theoretical linewidth expression given by Eq. (3.35) for comparison with the measured FWHM of the Stokes TA(2-2′) components. These comparisons showed that for $\omega < \omega_T$ a value of Γ between 0.3 and 0.5 cm^{-1} might be appropriate. However, in the frequency region between ω_T and ω_L, the observed FWHM of the TA lines increases monotonically. A similar trend was also observed for the Stokes LA(2-2′) components. Cho[24] has suggested that for branch-two polaritons near resonance ($\omega_T \leq \omega \leq \omega_L$), new decay channels may come into effect due to the increase in momentum. This would then result in an increase of Γ with increasing frequency, in qualitative agreement with our FWHM data. Alternatively, the increased linewidth may be due to attenuation of acoustic phonons which is expected to increase with increasing Brillouin shift. [This contribution to Δ was dropped at Eq. (3.32).]

There is, however, a more disturbing problem concerning Γ. Our Brillouin linewidth measurements indicate $\Gamma \sim 0.3$ cm^{-1} in the resonance region and our absorption measurements indicate a lower limit of ~ 0.05 cm^{-1}. However, direct polariton fluorescence measurements on similar crystals by Yu[25] give $\Gamma \sim 0.01$ cm^{-1}, close to the value determined by Flynn and Geschwind from their Brillouin linewidth measurements.[18] A possible though untested explanation for this discrepancy is that elastic scattering of polaritons from defects or dislocations would contribute to both attenuation and Brillouin linewidth by effectively removing polaritons from the initial or final mode $\vec{k}_i$ or $\vec{k}_s$, but would not reduce the polariton life-

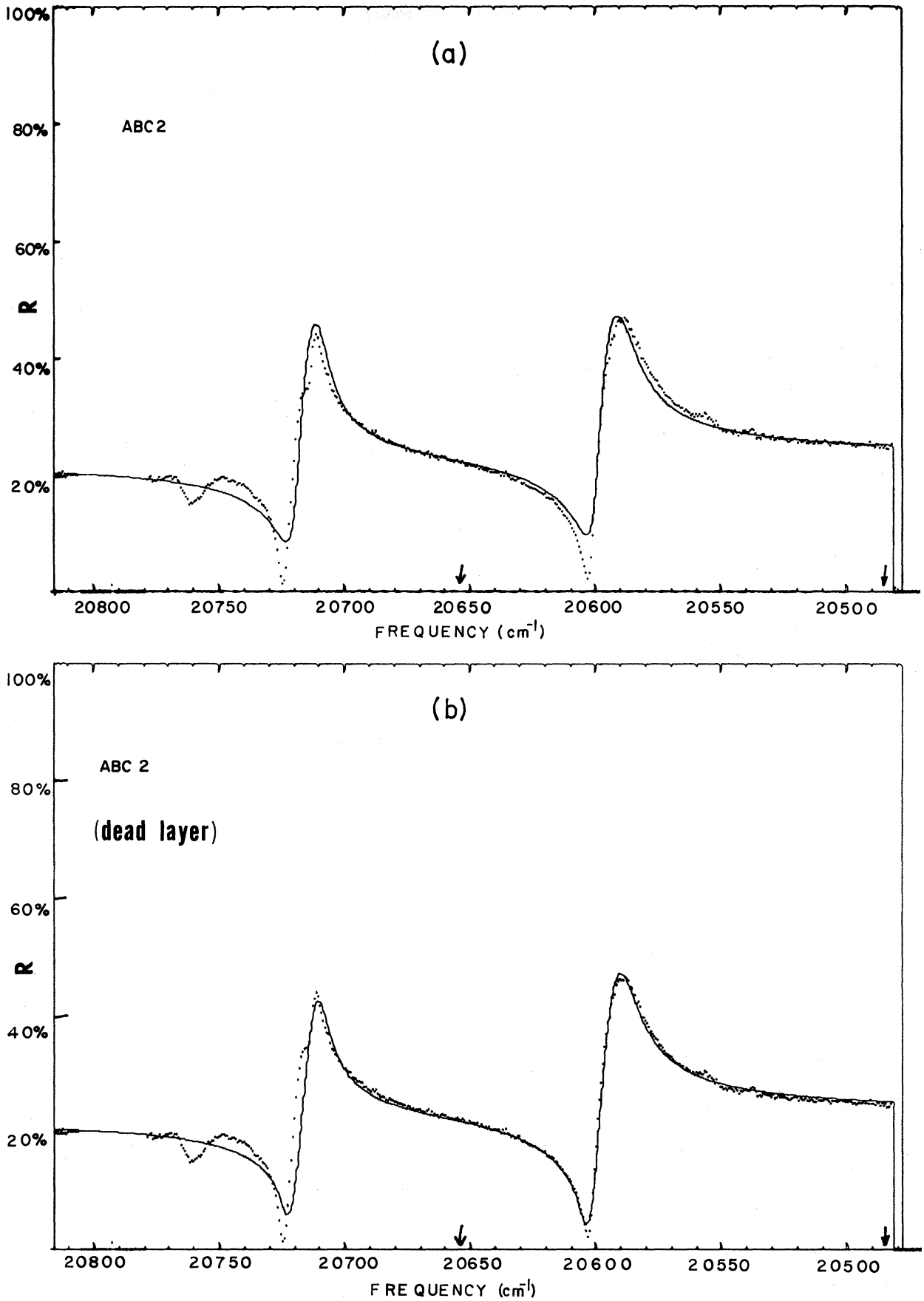

FIG. 12. Nonlinear least-squares fit of the theoretical reflectivity (solid lines) using ABC2 to the experimental reflectivity data (a) without a dead layer, and (b) with a dead layer included. The arrows indicate the frequency region in which fitting was taking place.

TABLE II. Best-fit values resulting from reflectivity analysis for each of the three ABC's.

	ABC1	ABC2	ABC3
Without dead layer			
Γ	2.09 cm^{-1}	6.97 cm^{-1}	5.04 cm^{-1}
$\bar{\epsilon}_b$	9.54	11.02	10.17
With dead layer			
Γ	0.582 cm^{-1}	6.36 cm^{-1}	3.765 cm^{-1}
$\bar{\epsilon}_b$	8.79	7.46	7.41
l	162 Å	148 Å	112 Å
n	1.92	2.68	2.83

time measured by fluorescence. Presumably, Flynn and Geschwind used CdS samples with much less elastic scattering than ours, which is also consistent with the much smaller attenuation that they observed. We note that Hermann and Yu found Brillouin linewidths in CdSe qualitatively similar to our CdS results shown in Fig. 7, and even larger numerically.[26] They also attributed the linewidth to elastic scattering of excitons from defects for incident laser frequencies above ω_L.

The theoretical external differential scattering cross-section analysis utilized the values of the exciton parameters obtained from the Brillouin shift analysis. The value of Γ was taken to be 0.5 cm^{-1} as discussed above. The intensity measurements for both the Stokes LA(2-2′) and TA(2-2′) (Figs. 8 and 9, respectively), seem to be peaking around 20 585 cm^{-1} (just below ω_T) and then suddenly decrease with a possible shoulder occurring around ω_L. Because of this behavior, it is difficult to determine whether ABC2 or ABC3 gives the best agreement between theory and data although it can be seen that ABC1 gives the worst fit. Therefore, one can only conclude that the data in these two figures fall between the two theoretical curves using ABC2 and ABC3.

The implication of Fig. 10 is that the general trend of the Stokes LA(1-1′) Brillouin intensity versus incident frequency follows the theoretical predictions with *any* of the three ABC's. However, when normalized against the Stokes LA(2-2′) intensities of Fig. 8 (solid circles) one sees that the intensity ratio $I(1\text{-}1')/I(2\text{-}2')$ is about 100 times smaller than predicted. Since both processes are mediated by deformation-potential scattering, their relative strengths are governed by differences in transmissivity, exciton strength functions, energy and group velocities, and the real and imaginary parts of the polariton wave vectors [see Eq. (3.36) in the following paper]. The group (or energy) velocity is particularly significant because the inner-branch polaritons participating in (1-1′) scattering have very small velocities leading to a large predicted cross section since $v_{E_i}(\omega_I)$ and $v_{G_j}(\omega_s)$ both occur in the denominator of Eq. (3.36).

Comparisons between reflectivity measurements and theory showed that much better fits could be obtained when a dead layer was incorporated into the analysis, even though no reflectivity "spike" was observed near the ω_L frequency. With the dead layer included, a good fit between theory and experiment could be obtained for all the ABC's.

The discrepancies observed between data and theory for the RBS linewidth and intensity measurements might be reduced by incorporating the following modifications in the theoretical analysis.

(i) Utilizing a theoretical form of Γ which increases monotonically with frequency. A first approach might be to use a linear form, $\Gamma=a[1+b(\omega-\omega_T)]$ and fitting this to the linewidth data of the TA(2-2′) scattering (Fig. 7). If this form of Γ improves the comparison between theory and experiment for the linewidth, then it could also be utilized in the theoretical comparison with the RBS intensity measurements for LA(2-2′) and TA(2-2′) scattering (Figs. 8 and 9).

(ii) Incorporating a dead-layer effect into the theoretical construction of the external cross section as well as the slightly non-normal incidence employed in the RBS experiments. Nonlinear least-squares fit between this revised theoretical cross-section calculation and the measured Brillouin intensity data could then be made for each ABC. This type of analysis has already been done to some extent by Yu and Evangelisti.[9] These authors incorporated a lossy dead layer into their theory and, upon comparison with their measured data, found that ABC3 produced the best fit to the Stokes LA(2-2′) components. However, their intensity measurements were obtained using a grating spectrometer which has a much lower resolution than the triple-pass Fabry-Perot interferometer utilized in our RBS experiments and were limited to the Stokes LA(2-2′) Brillouin component.

(iii) The third possibility would be the utilization of a general form of ABC. Such a form has recently been presented by Halevi and Hernández-Cocoletzi in their analysis of CdS reflectivity data.[27] Our feeling is that reflectivity comparisons are not very useful in the determination of the proper ABC since we have obtained good fits using all three ABC's. However, the general form of ABC might be very useful in the RBS intensity comparisons.

We have initiated a new experimental and theoretical study in which these (and other) modifications will be incorporated in an attempt to rectify the large discrepancy between RBS theory and experiment. The results of this analysis will be presented in a planned future publication.

ACKNOWLEDGMENTS

We wish to acknowledge the participation of Dr. Emil Koteles, Dr. William Yao, and Dr. Richard Bruce in the early stages of this research. We also wish to thank Dr. D. C. Reynolds of Wright-Patterson Air Force Base Laboratory, Dr. W. A. Albens of General Motors, Dr. E. A. Fagen of the University of Delaware, and Dr. C. H. Henry of AT&T Bell Laboratories for generously providing the CdS platelets for these experiments. For many helpful and informative discussions we thank Dr. Claude Weisbuch, Dr. Rainer Ulbrich, Dr. Roland Zeyher, Dr. Peter Yu, Dr. Ashok Puri, and Dr. Martin Copic. We are particularly indebted to Professor Joseph L. Birman for suggesting this problem to us and for providing continuing advice and encouragement. This research was supported by the National Science Foundation under Grant No. DMR-80-20835.

*Present address: Physics Department, Brookhaven National Laboratory, Upton, NY 11973.

†Present address: Research Institute of Electrical Communication, Tohoku University, Sendai 980, Japan.

‡Permanent address: Department of Engineering Physics, University of Electro-Communications, 1-5-1 Chofugaoka, Chofu-shi, Tokyo 182, Japan.

[1]S. I. Pekar, Zh. Eksp. Teor. Fiz. 33, 1022 (1957) [Sov. Phys.—JETP 6, 785 (1958)]; 34, 1176 (1958) [34, 813 (1958)].

[2]J. J. Hopfield, Phys. Rev. 112, 1555 (1958).

[3]*Excitons,* edited by E. I. Rashba and M. D. Sturge (North-Holland, Amsterdam, 1982).

[4]W. Brenig, R. Zeyher, and J. L. Birman, Phys. Rev. B 6, 4617 (1972).

[5]B. Bendow and J. L. Birman, Phys. Rev. B 1, 1678 (1970).

[6]P. Y. Yu, in *Light Scattering in Solids,* edited by J. L. Birman, H. Z. Cummins, and K. K. Rebane (Plenum, New York, 1979), p. 143.

[7]R. G. Ulbrich and C. Weisbuch, *Festkorperprobleme XVIII—Advances in Solid State Physics,* edited by J. Treusch (Vieweg, Braunschweig, 1978), p. 217.

[8]E. S. Koteles, in *Excitons,* edited by E. I. Rashba and M. D. Sturge (North-Holland, Amsterdam, 1982), p. 83.

[9]P. Y. Yu and F. Evangelisti, Phys. Rev. Lett. 42, 1642 (1979).

[10]J. Wicksted, M. Matsushita, and H. Z. Cummins, Solid State Commun. 38, 777 (1981).

[11]A. S. Pine, Phys. Rev. B 5, 3003 (1972).

[12]R. H. Bruce and H. Z. Cummins, Phys. Rev. B 16, 4462 (1977).

[13]G. Winterling and E. S. Koteles, Solid State Commun. 23, 95 (1977).

[14]P. Y. Yu and F. Evangelisti, Solid State Commun. 27, 87 (1978).

[15]G. Winterling, E. S. Koteles, and M. Cardona, Phys. Rev. Lett. 39, 1286 (1977).

[16]E. S. Koteles and G. Winterling, Phys. Rev. Lett. 44, 948 (1980).

[17]J. J. Hopfield and D. G. Thomas, Phys. Rev. 132, 563 (1963).

[18]E. J. Flynn and S. Geschwind, Bull. Am. Phys. Soc. 26, 488 (1981).

[19]I. Broser and M. Rosenzweig, Solid State Commun. 36, 1027 (1980).

[20]M. Rosenzweig, Ph.D. thesis, Technischen Universität Berlin, 1982.

[21]The collection aperture at the camera lens (L_2) subtended a half angle of $\sim 6°$ at the crystal. In the resonance region the refractive index is $n \sim 10$, so the range of internal scattering angles was $\sim 180° \pm 0.6$ giving a range in $\sin\theta/2$ of $< 2 \times 10^{-5}$. Therefore, instrumental linewidth due to finite collection aperture was less than 2×10^{-5} of the Brillouin shift.

[22]H. Z. Cummins and R. H. Bruce, Bull. Am. Phys. Soc. 22, 436 (1977).

[23]G. Winterling and E. S. Koteles, in *Lattice Dynamics,* edited by M. Balkanski (Flammarion, Paris, 1978), p. 170.

[24]K. Cho (private communication).

[25]P. Y. Yu (private communication).

[26]C. Hermann and P. Y. Yu, Solid State Commun. 28, 313 (1978); Phys. Rev. B 21, 3675 (1980).

[27]P. Halevi and G. Hernández-Cocoletzi, Phys. Rev. Lett. 48, 1500 (1982).